International Journal of Signal Processing, Image Processing and Pattern Recognition
Vol.9, No.7 (2016), pp.315-328
http://dx.doi.org/10.14257/ijsip.2016.9.7.28

A Novel Approach to Generate Chirped Waveform by using Chirped Lithium Niobate Mach-Zehnder Modulator

Akash Srivastav[1]* and Sanjeev Kumar Raghuwanshi[2]

Electronics Engineering Department, Indian School of Mines Dhanbad, Jharkhand-826004, India
** akash2011srivastav@gmail.com*

Abstract

A novel technique to generate an arbitrary chirped waveform by harnessing features of Lithium Niobate ($LiNbO_3$) *Mach-Zehnder analog intensity Modulator is suggested and verified by mathematical analysis. The most important application of chirped microwave waveform is that, it improves the range- resolution of radar. In the proposed approach, two electrical drive signal of opposite gain is used to modulate light coming out from the continuous-wave (CW) laser in* $LiNbO_3$ *Mach-Zehnder modulator (MZM). The output of the MZM is chirped optical waveform due to the dependence of the mach-zehnder modulators chirp on the form of signals applied to the drive electrode. In our simple and straight forward method of producing chirped waveform, is basically based on the concept of change in phase at the two arms of Lithium Niobate*($LiNbO_3$) *Mach-Zehnder modulator due to change in refractive index at the respective arms when electric drive voltage is applied. The chirping phenomenon is expressed in terms of an intrinsic chirp parameter* α_0 *of the MZM. The proposed design is simple, easy to implement and cost effective than the previously proposed model of chirped waveform generation uses the MZM and chirped fiber Bragg grating.*

Keywords: *Fiber Bragg Grating(FBG) Mach Zehnder Modulator(MZM) , Range Resolution*

1. Introduction

Microwave photonics is pertaining to multiple distinct fields of study that studies the interact between the field of microwave and optical signals, for applications such as broadband wireless access networks, sensors networks, satellite communications, instrumentation as well as warfare systems. From last few years people works immensely to research new microwave and photonics techniques for various applications. The major function of microwave and photonics system includes photonic generation, processing, control and distribution of microwave and millimeter (mm-wave) signals [1]. Normally microwave photonics systems are designed to operate at the 1550nm band in order to take advantage of attenuation [2]. This paper is focused on generating an arbitrary chirped waveform in optical domain. Basically a chirp signal is usually referred as a sinusoidal signals whose frequency increases or decreases with respect to time. These signals are frequently used in earth remote sensing (synthetic Aperture Radar-SAR, RADAR-Altimeter-RA), Planetary remote sensing as well as required for several application like target velocity estimation, acoustic digital imaging and the determination of system response with network analyzer [3].

*Corresponding Author

ISSN: 2005-4254 IJSIP

2. Photonic Microwave Arbitrary Waveform Generation Technique

The fundamental process to generate a microwave arbitrary waveform is Optical pulse shaping, so we are focusing to generate Arbitrary microwave chirped waveform based on optical pulse shaping [4] .The techniques implemented using pure fiber optics offer advance features of small size, lower loss, better stability and high potential for integration when compared with those implemented using free space optics [5]. Here we are presenting a chart in Figure1 that is showing various techniques for generating a photonic microwave arbitrary waveform. Finally we used a concept of optical pulse shaping for the generation of chirped waveform due to its advancement and easiness, by using a $LiNbO_3$ Mach Zehnder Modulator which acts as an optical pulse shaper. Beside optical pulse shaping technique some other techniques also include the generation of chirped microwave pulses like wavelength to time mapping and photonic microwave delay line filter [6]. In an optical spectral shaping and wavelength to time mapping for generation of chirped microwave arbitrary waveform by shaping the spectrum of an ultra-short optical pulse with a filter (usually FBG) that have a capacity to linearly increase or decrease the free spectral range (the frequency space between two consecutive transmission peak) and the spectrum shaped pulse is then linearly mapped to the time domain in dispersive element [7].

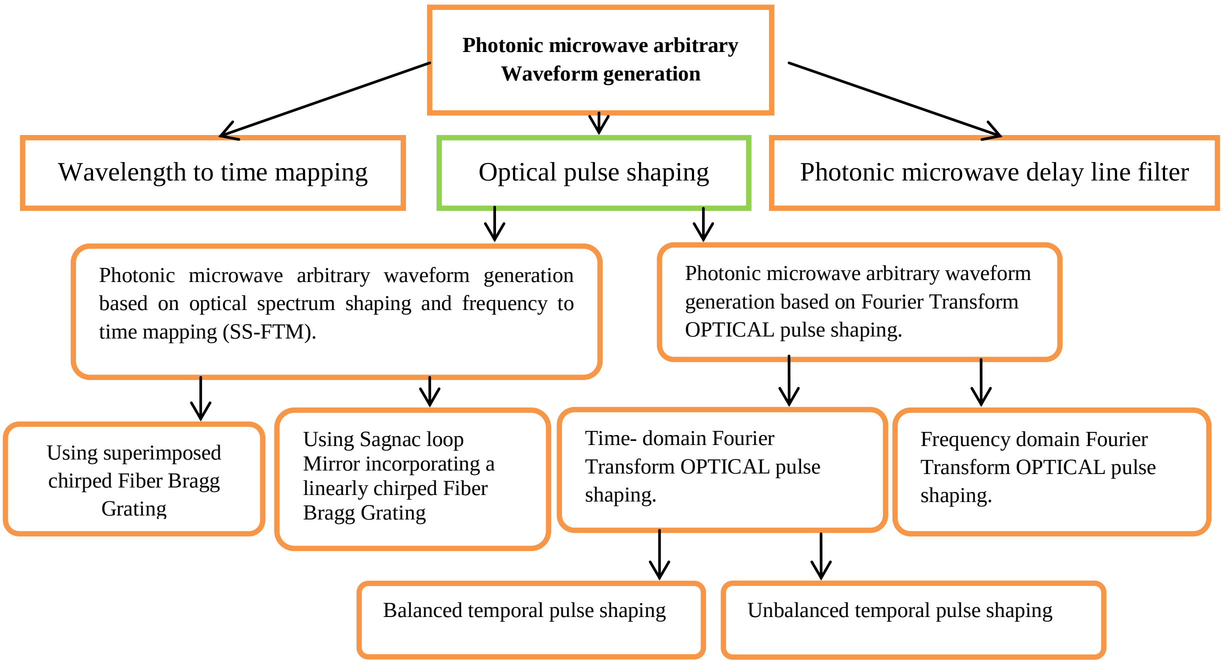

Figure 1. Different Techniques to Generate Chirped Microwave Arbitrary Waveform Based on Optical Pulse Shaping

The above chart gives a basic knowledge to generate an arbitrary microwave waveform by different methods. Millimeter wave (mm-wave) and microwave have the property of high frequency and large bandwidth that’s why these techniques have become an important research area that has a number of scientific and industrial application such as Ultra Wide band and multiple access communication system, pulsed Radar system etc[8].

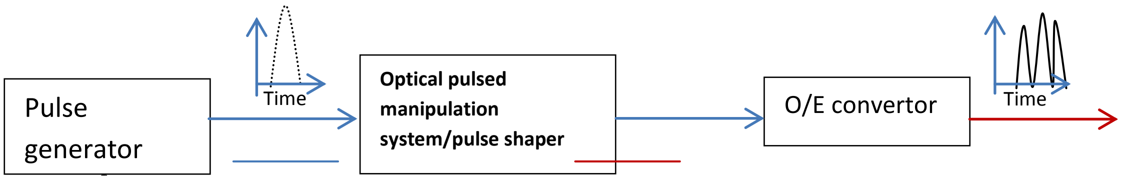

Figure 2. Basic Block Diagram of Optical Pulse Shaping for Arbitrary Microwave Waveform Generation

The advantages of pulse shaping involve control on amplitude, phase, and frequency and/or interpulse separation. Complex pulse shaping allows generation of ultrafast optical waveform according to user specifications. The above Figure2 shows the general structure of photonically assisted microwave arbitrary waveform generation. An ultra-short non-continuous optical pulse from a pulsed laser source is fed to a properly designed optical pulse manipulation system or pulse shaper, where the optical pulse is shaped in the optical domain here the pulse shaper will be treated as optical modulator and the input pulse will be multiplied with a modulating function. The modulating function in optical pulse modulator will be in time domain or frequency domain (obtained by Fourier transform)[9]. A microwave waveform with the desired shape is finally obtained after the optical to electrical conversion with the help of photo detector. The frequency of receive microwave waveform at output is limited by the bandwidth of the PIN Diode.[10]

3. Experimental Setup

A. Operating Principle

The complete experimental setup to generate the chirped arbitrary microwave waveform in optical domain is shown in Figure3. It has one non return to zero pulse generator [9] followed by a user defined bit sequence generator [10]. The NRZ pulse generator generates a sequence of non-return to zero pulses coded by an input digital signal. It shapes the input digital signal to a Not Return to Zero electrical signal .The output of the NRZ-PG is given to a low pass Bessel filter which provides a maximally flat group delay or propagation delay across the frequency spectrum [11]. Since the Bessel filter have advancement over other filter that it gives better shaping factor, flatter phase delay, and flatter group delay that's why we have preferred the Bessel filter in our experimental setup. Another advantage to use the filter is that it preserves the wave shape of the filtered signal in pass band [12]. After filtering, the signal is divided into two parts by the use of an electrical splitter for further modulation of the signal [13]. The first arm of the splitter provide the signal to the first port of the Mach Zehnder Modulator(MZM) and the signal through second arm is fed into second port of the modulator by passing through the negative gain provider. Two electrical signal of opposite gain are given to MZM for generating the chirp signal which is further being superimposed over continuous wave laser output for getting chirp signal in optical domain. It should be noted that we have used a $LiNbO_3$ based MZM which plays a vital role to control the amplitude of the optical wave [15]. The MZM also used to benefits of pulse compression to the system, thereby offering a reduced dispersion penalty compared to chirp free waveguide modulator. Here the MZM consist of an input Y branch waveguide, two phase modulated arms with independent drive electrodes and output Y branch waveguide for recombining the output from the phase modulated arms.

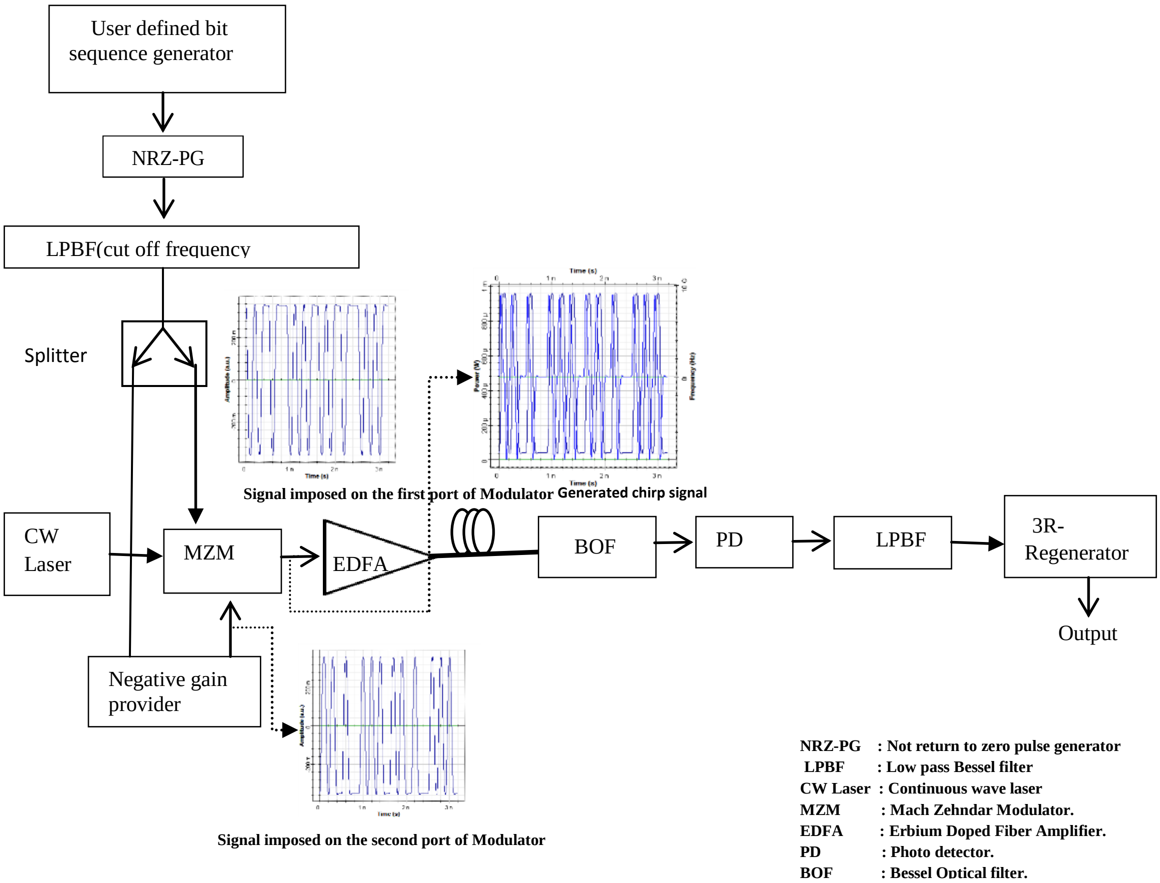

Figure 3. Complete Experimental Setup to Generate the Chirped Waveform Signal in Optical Domain

The modulated signal is further amplified by Erbium Doped Fiber Amplifier (EDFA)[16] and passes through single mode fiber (ITU's G.655[17].The use of the erbium doped fiber amplifier has drastically changed the technological issue of long-haul fiber transmission. No longer is the transmitter/receiver power budget the primary concern, but rather fiber dispersion, fiber non-linearties and amplifier noise are key factors. Now the signal further filtered out by the use of Bessel Optical Filter and after passing through the photo detector the signal is converted into electrical signal. This electrical signal passes though the low pass Bessel filter (LPBF) where the signal higher from cutoff frequency is omitted. At last the signal fed into the 3R-Regenerator where re-amplification, re-shaping, and re-timing of the signal occurs [18].

B. Mathematical Analysis.

As shown in the above Figure 3 a user defined bit sequence generator generate a bit sequence of 16 bit length as 0101 1011 1010 1011 with bit rate of 10Gbps is given to NRZ-PS where NRZ-PS generates the non-return to zero coded electrical signal. The signal further forward to low pass Bessel filter having cutoff frequency of 7.5 GHz .The signal after LPBF is further splitted out into two parts to provide input to the two arm of $LiNbO_3$ MZM. A continuous light wave from laser [$E_C \cos\omega_C t$ where E_c is the amplitude of optical field and ω_c is angular frequency of optical carrier] is given to the MZM [19]

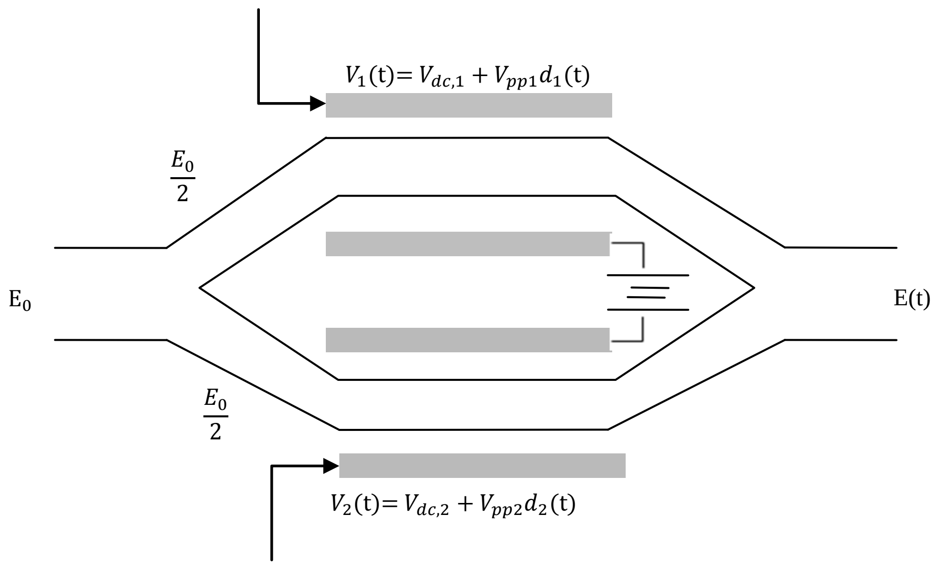

Figure 4. Structure of Mach-Zehnder Modulator

In order to illustrate the operating principle of such a device, the simple interferometry structure is represented in Figure4. It is based on a Mach-Zehnder interferometer including one electro-optic material in one of the arms [20]. When used as a data modulator, such a structure is generally integrated by diffusing some waveguides in the electro-optic material and depositing the electrodes on top or around the waveguides. Assuming the power is split or combined equally at the input and output couplers of the Mach-Zehnder interferometer, the power at the output of the interferometer depends on the difference between the phase shifts experienced by the light propagating in the upper and lower arm of the structure, $\phi(t)$and ϕ_0, respectively, according to:

$$P_{out} = P_{in}\cos^2(\Delta\phi)$$

Where $\Delta\phi = \phi(t) - \phi_0$. Lithium-Niobate($LiNbO_3$) is customarily used as a suitable electro-optic material for high-speed modulation inoptical communication systems, owing to its relatively large electro-optic coefficient and wellcontrolled waveguide fabrication processes. Applying a half wave voltage voltage of V_π to the electrode of an electro-optic waveguide will result in a voltage induced phase shift of π. The electro-optically induced phase shift ϕ (t) can therefore be related to the applied voltage V (t) according to:

$$\phi\ (t) = \pi\frac{V(t)}{V_\pi}$$

Assume that the input optical beam of amplitude E_0 and frequency ω_0 is splitted between the two arms and after travelling through the arms of modulator the output of modulator is expressed as the sum of the contributions propagating through the upper and lower paths.

$$E(t) = E_1(t)+E_2(t)$$

$$= \frac{1}{2}E_0[e^{j(\omega_0 t+V_{\gamma1}V(t)+\ \varphi_{D1})}+e^{j(\omega_0 t+V_{\gamma2}V(t)+\ \varphi_{D2})}] \quad (1)$$

Where, $\varphi_{D1}$and φ_{D2} are the static phases for arm1 and arm2 of MZM

$V_{\gamma1}$and$V_{\gamma2}$ are the voltage to phase conversion coefficient for arm1 and arm2, which is assumed to be constant with respect to the applied modulating voltage V(t).

In case of no modulation, a dc bias voltage controls the static phase difference $\Delta\varphi_D \equiv \varphi_{D1} - \varphi_{D2}$ and thus determines the output intensity. Meanwhile, when modulation is applied, the output field can be expressed as:

$$E(t) = E_0\cos(\Delta\varphi_D(t)).e^{j(\omega_0 t+\varphi(t))} \quad (2)$$

Where, $\Delta\varphi_D(t) = \frac{1}{2}[(V_{\gamma 1}.V(t)+\varphi_{D1}) - (V_{\gamma 1}.V(t)+\varphi_{D2})]$ (3)

And $\varphi(t)= \frac{1}{2}[(V_{\gamma 1}.V(t)+\varphi_{D1}) + (V_{\gamma 1}.V(t)+\varphi_{D2})]$ (4)

Equation (4) is basically the expression of output electric field at MZM in terms of the time dependent phase difference $\Delta\varphi_D(t)$ and time dependent output phase$\varphi(t)$.
The optical power at MZM's output is:

$$P(t)=\sqrt{\frac{\epsilon}{\mu}}|E(t)|^2= P_{in}\cos^2(\Delta\varphi_D(t)) \quad (5)$$

Where $P_{in} = \frac{1}{2}\sqrt{\frac{\epsilon}{\mu}}E_0{}^2$, is the optical power at the input of MZM, ϵ and μ are the permittivity and the permeability of the medium.
In the coming section, we will briefly describe the loss modulator and there after the derivation of the expression for chirp in modulated light frequency in a lossy modulator[23-24] .Suppose that the input light into the modulator has a constant amplitude E_0 and constant angular frequencyω_0, the amplitude E and the phase φ of the input light are given by:

$E = E_0 e^{j(\omega t-\beta L)}$
$= E_0 e^{j(\omega t-k_0 nL)}$
$= E_0 e^{j(\omega t-k_0(n'-jn'')L)}$, where refractive index of loss modulator, *i.e.*, $n = n' - jn''$
$= E_0 e^{j(\omega t-k_0 n'L)}.e^{(-k_0 n''L)}$

$$|E| = E_0\exp(-k_0 n''L) \quad (6)$$

And, $\varphi = -k_0 n'L$ (7)

where L is the length of an external modulator and k_0 is the propagation constant is free space.

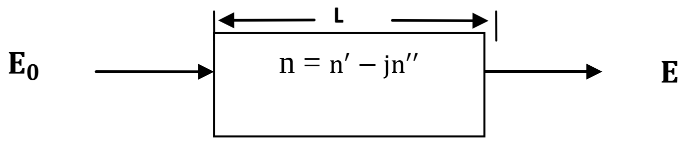

Figure 2. Overview of An External Loss Modulator

n': The real part of refractive index responsible for phase modulation.
n'': The imaginary part of refractive index responsible for intensity modulation.

Rate of change of phase with respect to time is:

$\frac{d\varphi}{dt} = - k_0 L\frac{dn'}{dt}$

or $= - k_0 L\Delta n'$ (8)

where$\Delta n' = \frac{dn'}{dt}$

Similarly, $\frac{dE}{dt} = E_0\exp(-k_0 n''L). (-k_0 L\frac{dn''}{dt})$

or

$= E.(-k_0 L). \Delta n''$ (9)

where, $\Delta n'' = \frac{dn''}{dt}$

From equation (9) we get: $k_0L = \frac{-1}{E}\frac{dE}{dt}\left(\frac{1}{\Delta n''}\right)$ (10)

From equation (8) and (10) we get:

$$\frac{d\varphi}{dt} = \frac{\Delta n'}{\Delta n''} * \frac{1}{E} * \frac{dE}{dt}$$

or $\frac{d\varphi}{dt} = \alpha.\left(\frac{1}{E}\right).\frac{dE}{dt}$

where α is the relative change of the real part $\Delta n'$ and imaginary part $\Delta n''$ of the refractive index ,*i.e.* $\alpha = \frac{\Delta n'}{\Delta n''}$

$$\text{or}\ \alpha = \frac{\frac{d\varphi}{dt}}{\left(\frac{1}{E}\right).\frac{dE}{dt}} \quad (11)$$

Now, we will define the intrinsic chirp parameter,

$$\alpha_0 = \frac{\frac{d\varphi(t)}{dt}}{\frac{d\Delta\varphi_D(t)}{dt}} \quad (12)$$

where α_0 is the ratio of the time derivative of the output phase $\varphi(t)$ to the time derivative of the phase difference $\Delta\varphi_D(t)$.

Note, $\varphi(t)$ is responsible for phase modulation and $\Delta\varphi_D(t)$ is responsible for intensity modulation.

After differentiating equation (3) and (4) with respect to time ‘t’ we get:

$$\frac{d\Delta\varphi_D(t))}{dt} = \frac{1}{2}[V_{\gamma 1}.\frac{dV(t)}{dt} - V_{\gamma 2}.\frac{dV(t)}{dt}] \quad (13)$$

$$\frac{d\varphi(t)}{dt} = \frac{1}{2}[V_{\gamma 1}.\frac{dV(t)}{dt} + V_{\gamma 2}.\frac{dV(t)}{dt}] \quad (14)$$

From equation (12), (13) and (14) we get:

$$\alpha_0 \equiv \frac{V_{\gamma 1}+V_{\gamma 2}}{V_{\gamma 1}-V_{\gamma 2}} \quad (15)$$

Thus, from equation (15) it is evident that the intrinsic chirp parameter is independent of the amplitude of the electric drive signal and thus it is an intrinsic parameter of the modulator.

Case(1): $\alpha_0 = 0$, *i.e.* $V_{\gamma 2} = -V_{\gamma 1}$, means pure intensity modulation

Case(2): $\alpha_0 = \infty$, *i.e.* $V_{\gamma 2} = V_{\gamma 1}$, means pure phase modulation

Case(3): $\alpha_0 = 1$, means electric signal is given to only one arm of MZM and hence modulation takes place in only one arm.

The amplitude of optical field at the output of Mach-Zehnder modulator is modulated according to $\Delta\varphi_D(t)$ and the output optical phase is modulated according to $\varphi(t)$. The variation in output optical pulse with time is related to the modulated phase $\varphi(t)$ by:

$$f(t) = \frac{1}{2\pi}\frac{d\varphi(t)}{dt} \equiv \frac{1}{2\pi}\frac{V_{\gamma 1}+V_{\gamma 2}}{2}.\frac{dV(t)}{dt} \quad (16)$$

Taking time derivative of equation (3) and (5) we get:

$$\frac{d(\Delta\varphi_D(t))}{dt} \equiv \frac{d}{dt}[\cos^{-1}(\sqrt{\frac{P(t)}{P_{in}(t)}})] \quad (17)$$

$$\text{And,}\ \frac{d(\Delta\varphi_D(t))}{dt} \equiv \frac{(V_{\gamma 1}-V_{\gamma 2})}{2}.\frac{dV(t)}{dt} \quad (18)$$

$$\text{Therefore,}\ \frac{d(\Delta\varphi_D(t))}{dt} \equiv \frac{(V_{\gamma 1}-V_{\gamma 2})}{2}\frac{dV(t)}{dt} \equiv \frac{d}{dt}[cos^{-1}(\sqrt{\frac{P(t)}{P_{in}(t)}})] \quad (19)$$

From equation (12), (16) and (19), the time varying frequency of the light pulse can write as:

$\frac{d\varphi(t)}{dt} = \alpha_0 \frac{d(\Delta\varphi_D(t))}{dt}$, and $f(t) = \frac{1}{2\pi}\frac{d\varphi(t)}{dt} = \frac{\alpha_0}{2\pi}\frac{d(\Delta\varphi_D(t))}{dt}$

$$f(t) = \frac{1}{2\pi}\alpha_0 \frac{d}{dt}(\cos^{-1}(\sqrt{\frac{P(t)}{P_{in}(t)}})) \quad (20)$$

Now, the frequency chirp of the light pulse is:

$$\frac{df(t)}{dt} = \frac{1}{2\pi}\alpha_0 \frac{d^2}{dt^2}(\cos^{-1}(\sqrt{\frac{P(t)}{P_{in}(t)}})) \quad (21)$$

It is apparent from equation (21) that the frequency chirp is determined by the modulating electric drive signal and modified by the intrinsic chirp parameter of the modulatorα_0. The intrinsic chirp parameter α_0 is not the same as intensity dependent chirp parameterα. The parameter α reduces to α_0 only in the case where the power is modulated with small amplitude, *i.e.* $V_{\gamma1}, V_{\gamma2} \ll 1$ and assuming $\Delta\varphi_D = \frac{-\pi}{2}$, which corresponds to the maximum condition for small amplitude modulation.

Thus,

$$\alpha \cong \alpha_0 \equiv \frac{V_{\gamma1}+V_{\gamma2}}{V_{\gamma1}-V_{\gamma2}} \quad (22)$$

Now when the signal propagates through the fiber its power decreases exponentially with distance and this loss of optical fiber is the attenuation in this paper the attenuation of fiber is fixed to 0.1db/km, another factor which influence the amplitude of signal through fiber is dispersion which is fix here upto the value of 16.75 ps/nm/km

Table 1. Complete Detail of the Parameter used in Implemented Device in the Experimental Setup

Devices	Parameter	Value
1. User defined bit sequence	Bit stream Bit rate	0101101110101011 10 Gbps
2. Continuous wave laser	Frequency Power Line -width	193.1 THz 0dBm 0 MHz
3. Mach Zehndar Modulator.	Extinction ratio Operating frequency Operating Wavelength	15 dB 40 GHz 1550 nm
4 Erbium Doped Fiber Amplifier.	Length Core radius Er doping radius Er metastable lifetime Numerical aperture Er ion density Loss at 1550nm	5m 2.2 µm 2.2 µm 10ms 0.24 10e+024 /m^3 0.1 dB/m
5 Bessel optical filter	Frequency Bandwidth Sample rate	193.1 THz. 10GHz 500GHz

6 Photo-detector	Responsivity Dark current Center frequency Sample rate	1 A/W 10 nA 193.1 THz 1600GHz
7. Low pass Bessel filter.	Cut off frequency Insertion loss Order	0.75*bit rate=7.5GHz 0dB 4th
8. Single mode fiber	Length Reference wavelength Attenuation Dispersion Differential group delay	10km 1550 nm 0.1 dB / km 16.75 ps/nm/km 0.2 ps/km

4. Result and Simulation

To verify the feasibility of the setup, simulation is firstly demonstrated. In the simulation, a bit stream of 01011011 1010 1011 with bit rate of 10Gbps is generated from user defined bit sequence generator. A low pass Bessel filter with cutoff frequency 7.5 GHz has been used here. Now the splitter here divide the incoming signal equally in two part where the first part is used here as a input of first electrode of modulator and the second part is applied on the second electrode of MZM through the negative electric gain provider. The operating wavelength of the MZM is 1.55μm with standard single mode fiber. Adjustable chirp modulator with two independent drive electrode offer the flexibility of optimizing the chirp characteristic of modulated optical signal for Radar application. The generated chirp pulse shown in Figure .5 is captured by a sampling oscilloscope.

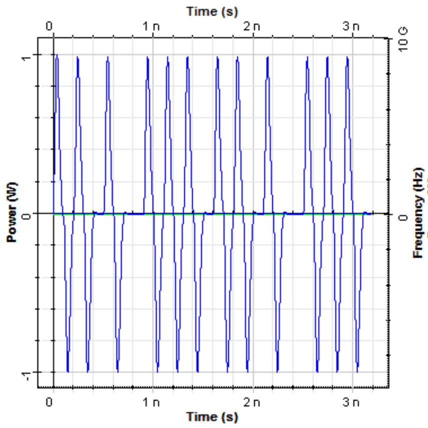

Figure 5. (a) Chirped Signal Generated Due to Two Electrical Drive Signal

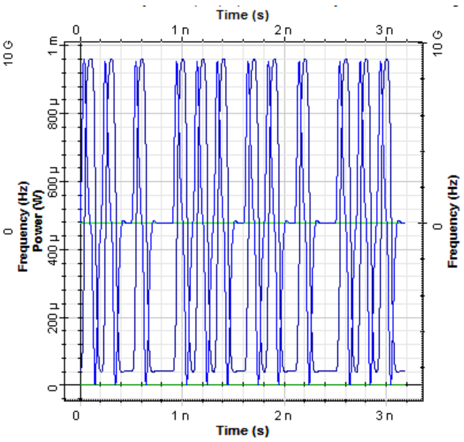

Figure 5. (b) Chirped Signal in Optical Domain by MZM

The above graph shows the comparative analysis of chirp signal in MZM before modulation and after the modulation. Figure5 (a) sows that the chirp signal generate within the MZM without superimposing it on the signal generated from CW Laser. On the other hand in the Figure 5(b) the signal on optical spectrum analyzer shows the signal having periodic variation with respect to time indicate the chirp signal in optical domain. In the coming section we have analyzed the different value of chirp parameter by taking different value of electrode voltage on MZM. The comparative study of different value of electrode voltage $V_{\gamma_1}, V_{\gamma_2}$ and their respective effect on the quality factor Q and chirp parameter α is in the table given below-

Case.1 When MZM electrode voltage V_{γ_1} is–ve and fixed to a particular value and V_{γ_2} is varied.

Table 2. Shows the Comparative Study of Different Value of Electrode Voltage at MZM Port and Respective Changes in Quality Factor and Attenuation Factor

V_{γ_1}	-5	-5	-5	-5
V_{γ_2}	1	2	3	4
Q	18.69 (Q_1)	12.48 (Q_2)	10.17 (Q_3)	3.32 (Q_4)
α	0.66	0.42	0.25	0.11

The value of Q is calculated by software and the value of α is calculated by the derived formula taken from eqn. 22. Here it is notice that$\frac{Q_1}{Q_2} = 1.49$,$\frac{Q_1}{Q_3} = 1.83$, $\frac{Q_1}{Q_4} = 5.62$

Case.2When MZM electrode voltage V_{γ_1} is +ve, $V_{\gamma_2}$is -ve and constant to a particular value.

Table 3. Shows the Comparative Study of Different Value of Electrode Voltage at MZM Port and Respective Changes in Quality Factor and Attenuation Factor

V_{γ_1}	1	2	3	4
V_{γ_2}	-5	-5	-5	-5
Q	27.89 (Q_1)	18.84 (Q_2)	9.10 (Q_3)	2.96 (Q_4)
α	-0.66	-0.42	-0.25	-0.11

$\frac{Q_1}{Q_2} = 1.48$,$\frac{Q_1}{Q_3} = 3.06$, $\frac{Q_1}{Q_4} = 9.42$

From the relative comparison of two tables its apparent that relative quality factor tends to decrease 5 times in table 1 when all value chirp parameter is +ve whereas in case 2 the relative quality factor tends to decrease approx. 10 times. So it's better to take the value of chirp parameter greater than zero and pick the value of MZM electrode voltage from table.1. Now in next step its clear from table .1 that the electrode voltage will be either (-5,1 or -5,2) because the value of quality factor is high only on these values. From the software analysis we reach on following conclusion-

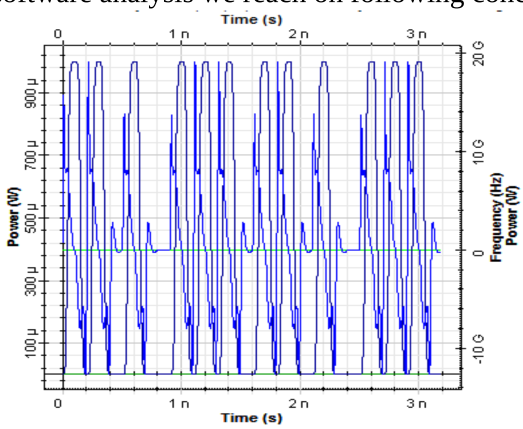

Figure 6. (a) Chirp Signal Output on Optical Spectrum Analyzer by Providing Electrode Voltage V_1= -5, V_2=1 of MZM

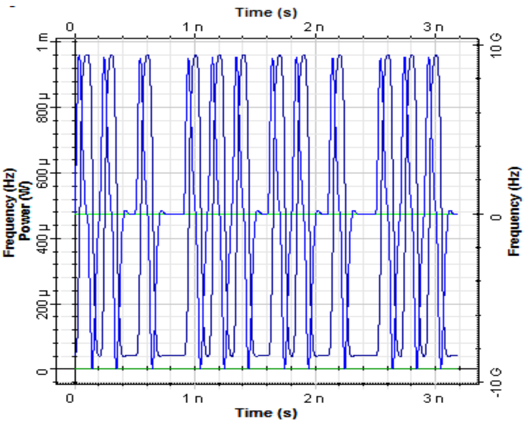

Figure 6. (b) Chirp Signal Output on Optical Spectrum Analyzer by Providing Electrode Voltage V_1= -5,

From the Figure (5).a and (5).b its apparent that the chirp signal appear on optical time domain visualizer is more clear and appropriate by giving the voltage value (-5,2) on the electrodes of MZM instead of (-5,1). Hence the chirp parameter of the signal will be 0.42 by taking V_{γ_1}= -5, V_{γ_2}=2. As the frequency of the CW laser is 193.1 THz so by calculation its evident that the wavelength of generated chirp signal will be approximately equal to 1550 nm. The signal lies in C band (1530 to 1560 nm) so to amplify it we use a EDFA. The optical amplifier increases the power level of incident light through stimulated emission. The next parameter of the amplifier is its gain, which increases with device length. In this paper the device length is taken as 5m. Here it's concluded that at 1550 nm wavelength the attenuation is very less[21] that's the resion of taking 1550 nm as reference wavelength. The supporting graph is shown in the Figure (6).

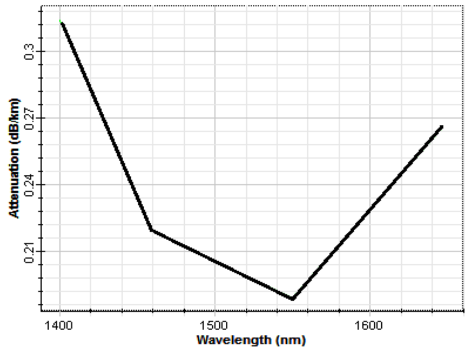

Figure 6. The Above Graph Shows that at 1550 nm Wavelength the Attenuation is Minimum

After amplification the signal is passed though the Bessel optical filter whose band-pass frequency is 193.1 THz and bandwidth is 50 GHz, now this band limited signal is given to photo-detector where the optical signal is converted to electrical domain. The signal further fed into low pass Bessel filter (LPBF) where the cut-off frequency of the filter is 7.5 GHz. The filter passes the signal with frequency lower than cut-off frequency and attenuates signal with frequency higher than certain cutoff frequency. The advantage of using the Bessel optical filter is that it provide maximum flat group/phase delay mean maximum linear phase response which preserves the wave -shape of filtered signal in pass-band.

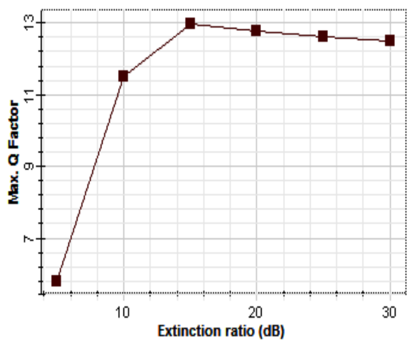

Figure 7.(a) Quality Factor vs. Extinction Ratio Graph

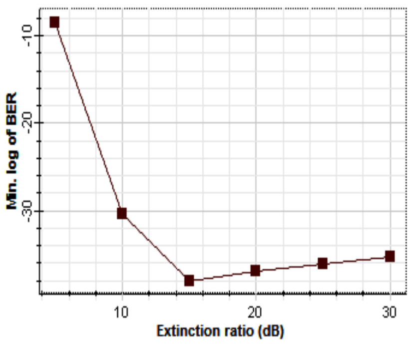

Figure 7.(b) Bit Error Rate vs. Extinction Ratio Graph

From the above Figure7 (a) its studied that the quality factor is maximum at the extinction ratio of 15dB and decreasing gradually after that. Another graph Figure (7).b shows that the bit error rate tends to decrease when we extend the value of extinction ratio and on the value of 14.5 dB the BER is minimum but as we increase the value of extinction ratio above 14.5 dB the BER tends to increase thus its concluded that the BER of the chirp signal is 12.483 and extinction ratio is14.5 db. Now in next section we have focused to get the effect of quality factor when we increase the length of fiber the graph given below shows the result obtained after simulation.

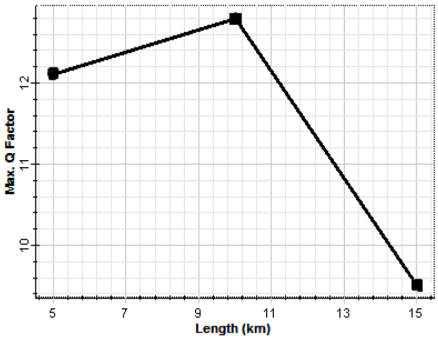

Figure 8. (a) Variation of Quality Factor with Respect to Length

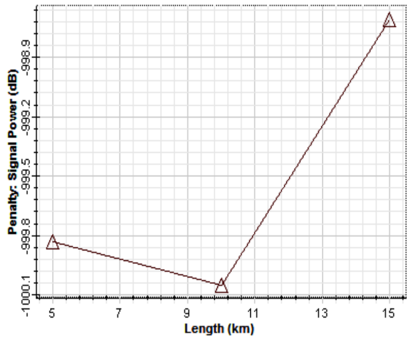

Figure 8. (b) Variation in Signal Power with Respect to Length

From the above Figure8(a) we have reached on the result that the quality factor of the signal increase gradually up-to 10km of the fiber length used but after this particular length the quality factor of the signal decreases abruptly. Before 10km attenuation does not have any major impact in deteriorating the quality of a signal because of the amplification of optical signal perform by EDFA. Meanwhile as we increase the value of fiber more than 10km the attenuation start playing a major role in decreasing the strength of optical signal. Now in Figure 8(b) we shows the effect on signal power obtained at the receiver after increasing fiber length. In Figure 8(a) it is concluded that at fiber length 10km the quality factor is maximum and graph Figure8 (b) shows that at 10km fiber length the power penalty is minimum and its evident that at this length of fiber the output SNR value will be maximum. Finally we have targeted to find the total bit error rate, eye diagram analysis and through it the quality factor of the signal. The graphical analysis is given below-

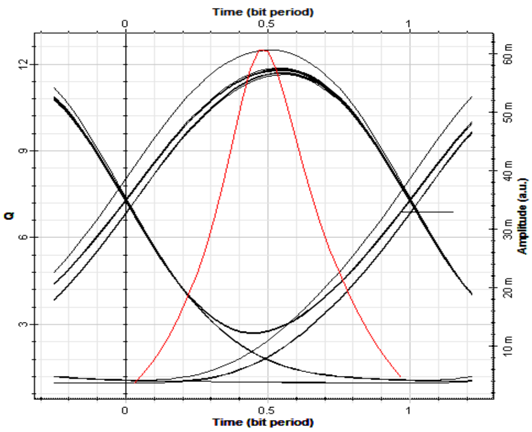

Figure 9. Simulated Eye Diagram of the Modulated Data at Output of OSA

The Q-factor performance, BER and eye patterns are discussed and analyzed in Figure 9. From above figure the result comes out that the quality factor of the signal is maximum at Bit period of 0.498 where the quality factor is maximum and bit error rate is minimum. The point where eye opening is maximum is best suited for safely sampling the signal with fidelity. This process is very important in 3R-generator because there re-amplification, re-shaping, and re-timing of the signal occurs.

5. Conclusion

Frequency chirping effect in external modulator *i.e.* $LiNbO_3$ Mach Zehnder modulator can be uniquely expressed by an equation in terms of α parameter. Different techniques to generate chirp microwave arbitrary waveform have been discussed via tabular form in which optical pulse shaping is adopted. The maximum quality factor of the signal is 12.483 at bit period of 0.498 at 10km fiber length.

References

[1] Yao, "Microwave Photonics, invited tutorial", JLT-10838, **(2008)**.
[2] L. Goldberg, H. F. Taylor, J. F. Weller and D. M. Bloom, "Microwave signal generation with injection locked laser diodes," Electron. Lett., vol. 19, no. 13, **(1983)**, June, pp. 491-493,
[3] P. Flandrin "Time-frequency and chirps"[online], available FTP :http://www.ens-lyon.fr/~flandrin/ (2007)
[4] A. M. Weiner, "Ultrafast optical pulse shaping: A tutorial review" Optics Communications ,ELSEVIER vol. 284, **(2011)**, pp. 3669–3692.
[5] M. Singh and S. K. Raghuwanshi, "Effect of higher order dispersion parameters on optical millimeter-wave generation using three parallel external optical modulators", Journal of Applied Physics (American Institute of Physics), vol. 117, no. 023116, **(2015)**.
[6] A. Malacarne1, S. Thomas, F. Fresi1, L. Potì, A. Bogoni and J. Azaña, "Programmable All-Fiber Optical Pulse Shaping", INTECH, Croatia, ISBN 978-953-7619-82-4, **(2010)**.
[7] A. J. Seeds and K. Williams, "Microwave photonics," J. Lightwave Technol., vol. 24, no. 12, **(2006)** December, pp. 4628-4641.
[8] C. Wang "Photonics generation of microwave arbitrary waveforms based on advance Fiber Bragg Gratings" Ph.D dissertation, department of information technology and engineering, University of Ottawa , Canada ,ISBN 978-0-494-79733-4, **(2010)**.
[9] M. Singh and S. K. Raghuwanshi, "Microwave generation analysis with higher order dispersion in two casca ded mach zehnder modulator", Optik (Elsevier), vol. 125, **(2014)**, pp. 761-771.
[10] J.S. Braley, A tutorial on photo detectors, available; http://www.ele.uri.edu/Courses/ele432/spring08/photo_detectors.pdf FTP:, **(2008).**
[11] Barry B. Brey "The Intel Microprocessors", 8th ed.: Pearson Prentice Hall. ISBN-13: 978-0-13-502645-8, ISBN: 0-13-502645-8, **(2008)**.
[12] A. Menezes, P. V. Oorschot and S. Vanstone, "Handbook of Applied Cryptography", CRC Press ,PP-169-190, ISBN: 0-8493-8523-7, **(1996)**.
[13] A. I. Zverev, "Handbook of Filter Synthesis", John Wiley, ISBN: 978-0-471-74942-4, **(1967)**.
[14] M. E. V. Valkenburg, "Analog Filter Design", Holt Saunders international edition, **(1982)**, pp. 279-291.
[15] J. C. Cartledge, "Performance of 10Gb/s light wave system based on lithium niobate Mach-Zehnder modulators with Asymmetric Y-Branch Waveguide" IEEE photonics technologletter, vol. 7, no. 9, **(1995)** September.
[16] A. Sheetal, A. K. Sharma and R. S. Kalerc, "Impact of extinction ratio of single arm sin2 LiNbO3 Mach–Zehnder modulator on the performance of 10 and 20 Gb/s NRZ optical communication system" Optik 120 704–709, ELSEVIER, **(2009)**.
[17] N. A. Mohammed, Y. E. Guindy and M. H. Aly, "System Optimization to Eliminate Chirping in Dual Drive LiNbO3 MZM at 40 Gb/s," ISSN: 2349-6495, vol-1, no. 2, **(2014)** July.
[18] G. Keiser, "Optical fiber communications", McGraw-Hill, **(2010)**.
[19] "Characteristics of a non-zero dispersion-shifted single-mode optical fibre and cable" ITU-T Recommendation G.655 link address http://www.thefoa.org/tech/SM%20fibre%20selection.pdf , **(2003)**.
[20] H. F. Chou and J. E. Bowers, "Simplified optoelectronic 3R regenerator using nonlinear electro-optical transformation in an electro absorption modulator", Optical Society of America, vol. 13, no. 7, **(2005)**.
[21] T. K. Ishii, "Handbook of Microwave Technology: Components and devices", Academic Press, 1995 ISBN 0-12-374696-5.
[22] A. Kumar Ghatak and K. Thyagarajan, "Optical Electronic", Cambridge University Press, **(1989)** July 20.
[23] G. E. Stillman, C. M. Wolfe, C. V. Bozler and J. A. Rossi, "Electro absorption in GaAs and its application to waveguide detector and modulator," Appl. Phys. Lett., vol. 28, **(1976)**, pp. 544-546.
[24] M. K. Sharma, H. Namizaki and S. Wang, "Monolithic integration of GaAs/GaAlAs light modulators and distributed Bragg reflector lasers," Appl. Phys. Lett., vol. 32, **(1978)**, pp. 314-316
[25] D. S. Chemla, T. C. Damen and D. A. B. Miller, "Electroabsorption by stark effect on room temperature exiton in GaAs/GaAlAs multiquantum well structure," Appl. Phys. Lett., vol. 42, **(1983)**, pp. 864-866.
[26] T. H. Wood, C. A. Burrus, D. A. B Miller, D. S. Chemla, T. C. Damen, A. C. Gossard and W. Wiegman, "131-ps optical modulator in semiconductor multi quantum wells(MQW's)," IEEE J. Quantum Electron., vol. 21, **(1985)**, pp-117-118.

[27] Y. Noda, M. Suzuki, Y. Kushiro and S. Akiba, "High-speed electro absorption modulator with strip-loaded GaInAsP planar waveguide," J. Lightwave Tech., vol. 14, **(1984)**, pp. 1445-1453.

